Table 1 Demographic data of the study participants

	Diagnostic group Normal control	AD alone	AD with DM
n	14	11	4
Sex (male/female)	7/7	4/7	2/2
Age	64.5 ± 2.9	78.5 ± 3.9	77.5 ± 5.2
MMSE	29.9 ± 0.1	20.5 ± 0.8	19.4 ± 2.8
ApoE ε4 allele (%)	0.12	0.35	0.37
HbA$_{1c}$ (%)	5.7 ± 0.1	5.8 ± 0.1	7.2 ± 0.4

AD, Alzheimer's disease; DM, diabetes mellitus; HbA$_{1c}$, glycated hemoglobin; MMSE, Mini-Mental State Examination.

In order to clarify etiology and dementia subtypes in diabetic patients, we took a unique approach to visualize amyloid β protein (Aβ) deposition by positron emission tomography (PET) in living diabetic patients with dementia. The Aβ accumulation is successfully and non-invasively visualized by a recently-developed novel amyloid imaging probe called BF-227.[27–31] We used this tracer and applied it to "diabetic" and "non-diabetic" patients with clinically-diagnosed AD, to obtain more insights into differences in the extent and distribution of Aβ accumulation between diabetic and non-diabetic groups.

Methods

A total of 14 normal controls (NC), four diabetic patients with AD (AD with DM) and 11 non-diabetic patients with AD (AD alone) were examined. All the dementia patients were clinically diagnosed as probable AD according to the clinical criteria by "the National Institute of Neurological and Communicative Disorders and Stroke – Alzheimer's Disease and Related Disorders Association".[32] Brain MRI (1.5 Tesla; General Electric, Fairfield, CT, USA) was carried out on all the participants to exclude other causes of dementia. All the DM types of diabetic patients with AD were type 2. The study protocol was approved by the Committee on Clinical Investigation at Tohoku University School of Medicine and the Advisory Committee on Radioactive Substances at Tohoku University. After a complete description of the study to the patients and subjects, written informed consent was obtained.

The PET procedure using BF-227 is described elsewhere.[28,31] BF-227 and its N-desmethylated derivative (a precursor of [11C]BF-227) were custom-synthesized by Tanabe R&D Service (Osaka, Japan) [11C]BF-227 was synthesized from the precursor by N-methylation in dimethyl sulfoxide using [11C]methyl triflate. The [11C]BF-227 PET study was carried out using a PET SET-2400W scanner (Shimadzu, Kyoto, Japan). After

intravenous injection of 211–366 mBq of [11C]BF-227, dynamic PET images were obtained for 60 min with each subject's eyes closed. Standardized uptake value (SUV) images of [11C]BF-227 were obtained by normalizing tissue radioactivity concentration by injected dose and bodyweight. Regions of interest (ROI) were placed on individual axial MR images in the cerebellar hemisphere, striatum, frontal, lateral temporal, medial temporal, parietal, occipital, anterior and posterior cingulate cortices. The ROI information was then copied onto dynamic PET SUV images, and regional SUV were sampled using Dr.View/LINUX software (AJS, Tokyo, Japan). Because there were neither senile plaques nor glucose hypometabolism in the cerebellum of AD patients, the ratios of regional SUV to cerebellar SUV (SUVR) were calculated as an index of [11C]BF-227 retention. Neocortical SUVR was calculated by averaging SUVR in the frontal, lateral temporal, parietal and posterior cingulate cortices. Apolipoprotein E genotyping was carried out as previously described.[33]

The difference of Neocortex SUVR between the group of AD with DM and other groups was assessed with Student's t-test. The performance of diagnostic indices to discriminate among groups was assessed using receiver operating characteristic (ROC) analysis. Areas under ROC curves (AUC) were calculated and compared using GraphPad Prism Software (GraphPad Software, San Diego, CA, USA). Statistical significance was defined as $P < 0.05$.

Results

The clinical features of the three groups, NC, AD alone and AD with DM, are described in Table 1. Severities of dementia assessed by Mini-Mental State Examination were not significantly different between AD alone and AD with DM. Three patients were treated with only oral DM medications (patient A glimepiride + pioglitazone; patient B glimepiride + metformin + voglibose; patient
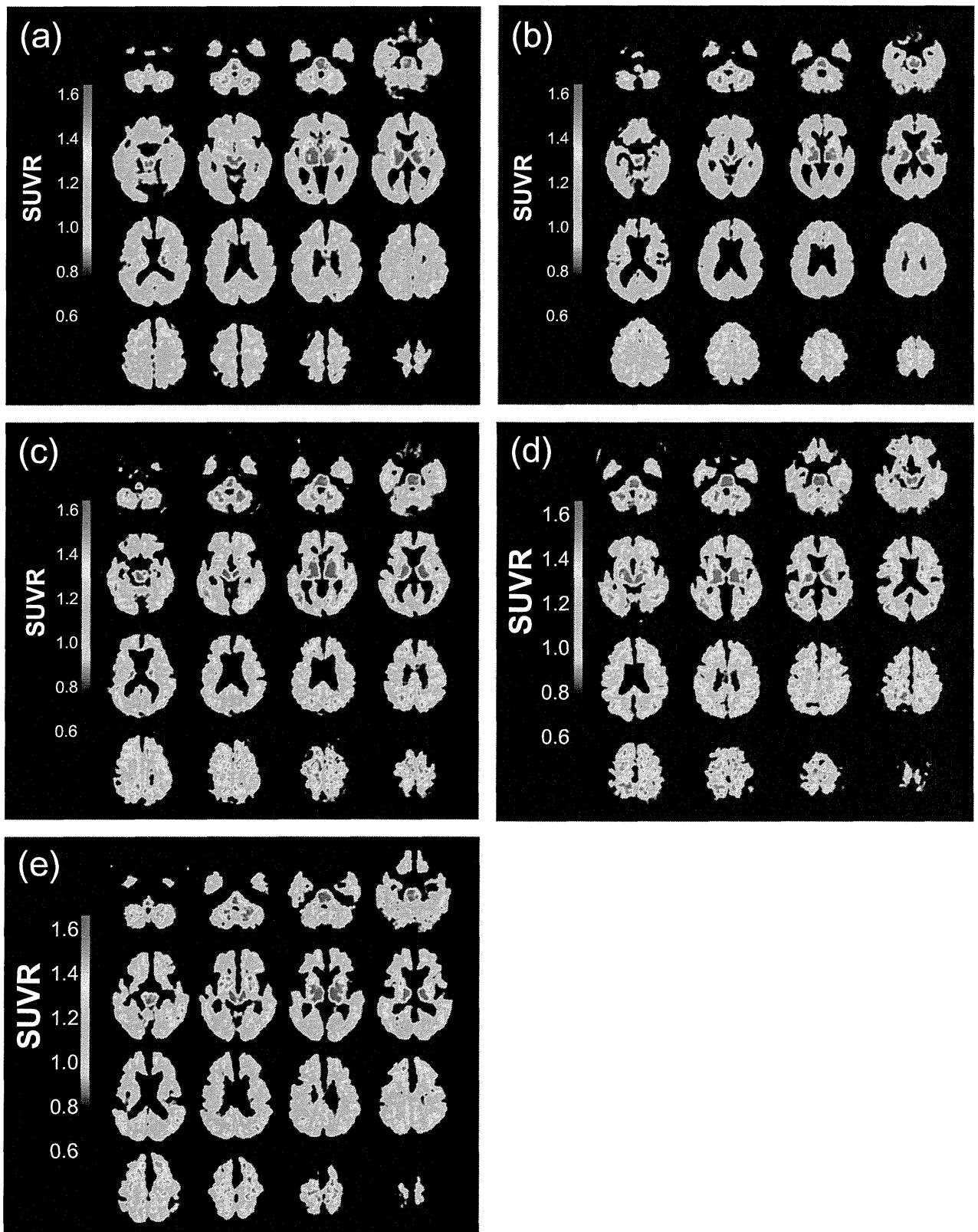
Figure 2 Representative BF-227 positron emission tomography images of each diagnostic group. (a) Normal control without diabetes mellitus (DM; 67-years-old, male, no complication; neocortical ratios of regional standardized uptake value to cerebellar standard uptake value ratio [SUVR] = 1.122). (b) Normal control with diabetes mellitus (67-years-old, female, insulin user; neocortical SUVR = 1.012). (c) Alzheimer's disease (AD) alone (75-years-old, female; neocortical SUVR = 1.230). (d) AD with DM (79-years-old, female, insulin user; neocortical SUVR = 1.240). (e) AD with DM (78-years-old, male, non-insulin user; SUVR = 1.18).
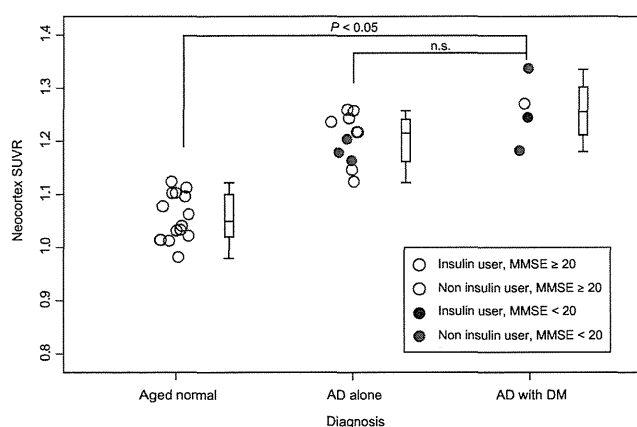
Figure 3 Box and scatter plots of ratios of regional standardized uptake value to cerebellar standard uptake value ration (SUVR) values with BF-227 in aged normal, Alzheimer's disease (AD) alone and AD with diabetes mellitus (DM) participants. Each circle indicates the mean SUVR from the mean neocortex. Red colored circle represents insulin user, whereas blue colored circle represents non-insulin user. There are no DM patients in the aged normal group shown with the blue circle. The filled circle represents the participants with Mini-Mental State Examination score less than 20. Although both AD with DM and AD alone showed significantly higher SUVR than the normal control group ($P < 0.05$), the difference between AD with DM and AD alone was not significant (n.s.).

Table 2 Characteristics of insulin users

	Subject 1 (no. 4) (normal cognition)	Subject 2 (no. 6) (AD patients)
Age	67	79
Sex	Female	Female
MMSE	28	21
ApoE genotype	3/3	3/3
CSF total tau (pg/ml)	–	334
BMI	24.7	19.8
HbA$_{1c}$ (%)	7.6	8.2
Medication	Insulin only	Insulin, metformin
Hypoglycemic event	several	none
Duration of insulin use (years)	11	7

AD, Alzheimer's disease; BMI, body mass index; CSF, cerebrospinal fluid; HbA$_{1c}$, glycated hemoglobin; MMSE, Mini-Mental State Examination.

C metformin + voglibose), whereas only one AD with DM patient used insulin in addition to metformin. One DM patient was present in the normal control group. This patient in the control group had no oral medication. Insulin injection was the only medication.

MRI scans showed no or very few ischemic or hemorrhagic lesions observed in any of the participants. These small lesions were not strategic. White matter lesions (both periventricular and deep white matter) are all less than mild according to the Fazekas criteria (data not shown).[34]

After we obtained demographic information, we analyzed PET images with BF-227 among the three groups, and representative brain PET images are shown in Figure 2. As indicated in the figure, both the patients with AD alone and AD with DM showed significantly more robust retention of BF-227 than NC. Statistical analysis showed a significantly higher SUV-R of BF-227 ($P < 0.05$) in the cerebral cortex of AD alone and AD with DM than NC, as shown in Figure 3. Neocortical SUV-R of BF-227 in AD alone and AD with DM are not significantly different. Both the patients with AD alone and AD with DM showed increased BF-227 uptake in frontal, temporal, parietal, occipital and cingulated gyrus. The pattern of uptake was similar between the DM patients with insulin use and those without the use of insulin (Fig. 2). A similar pattern of uptake between insulin users and non-insulin users was seen both in the control group and the AD with DM group.

The clinical profiles of the two insulin users are shown in Table 2.

Discussion

The present study had two major findings. First, the uptake of BF-227 was significantly higher in both AD groups than that of the normal control group, regardless of DM complication. Second, the amount and pattern of the uptake was not affected by the use of insulin, both in the control group and the AD with DM group.

The first result that the severity and extent of the deposition did not differ significantly between the two groups suggests that both AD with DM and AD alone have robust deposition of senile plaques or typical AD pathology. In addition, all the participants we examined showed no or very few vascular lesions observed with MRI, indicating that we could exclude vascular dementia. The present result showed that the cause of developing dementia in DM patients cannot be fully explained by vascular mechanism. From the results of previous studies,[13,14] we assumed that either extra or less deposition of amyloid plaques would be seen in the brain of AD patients with DM complication. However, the brains of AD patients with DM showed a similar pattern and severity of the amyloid deposition to that seen in the brains of AD without DM complication. One possible explanation is that some kinds of protein that cannot be detected by BF-227 play a more important role than the classical aggregated plaque. Soluble

| 219

Aβ oligomers, which cannot be detected by BF-227, were shown to lower insulin receptor responses to insulin and cause substantial loss of neuronal surface insulin receptors.[35] Another possibility is that the additional effect of DM complication appears mainly through the increase in phosphorylation of tau, instead of an increase of Aβ plaque.

The second result of AD patients is in conflict with those reported by Beeri *et al.*[18] According to their conclusion, the AD patient with insulin and metformin use (subject 4 in Fig. 2) should have shown fewer senile plaques (lower uptake) as compared with diabetic patients with other medication status or non-diabetic subjects. One explanation for this inconsistency is that he/she was an *APOE* ε4 non-carrier. The occurrence of neurofibrillary tangles and amyloid plaques in people without the *APOE* ε4 allele were similar to those with and without DM in the autopsy population of the Honolulu-Asia Aging Study.[12] It is assumed that the effect of insulin and other medication use on reducing the plaques might only be effective in reducing the extra deposition of amyloid plaques in *APOE* ε4 carriers.

It was also found that the insulin user with normal cognition (subject 2 in Fig. 2) showed no difference in uptake. This subject was not obese, and started insulin injections 11 years before she undertook the PET procedure. Her glycohemoglobin level was 7.6%, and she had experienced several hypoglycemic events just before participation in the present study. From these clinical features, we assume that one of the main components of her DM were fluctuations of her blood glucose level (hyperglycemia and hypoglycemia). The interaction with ApoE ε4 might also be thought to be an explanation.

A limitation of the present study was that we could not adjust some factors, such as age, due to the small sample size. Because of the small sample size, the present study should be treated as a preliminary report. In addition, we could not measure the value of their homeostasis model assessment ratio, which is one of the key indicators of insulin resistance. We could not measure this indicator of insulin users, because they already had started insulin before admission to our clinic. Further studies are required to clarify the present report.

In conclusion, the present study provided new and important preliminary findings that a similar pathomechanism, which is the deposition of robust aggregated Aβ in the brain, is shared in both AD with DM and AD alone.

Disclosure statement

The authors declare no conflict of interest.

References

1 Barnes DE, Yaffe K. The projected effect of risk factor reduction on Alzheimer's disease prevalence. *Lancet Neurol* 2011; **10**: 819–828.
2 Biessels GJ, Staekenborg S, Brunner E, Brayne C, Scheltens P. Risk of dementia in diabetes mellitus: a systematic review. *Lancet Neurol* 2006; **5**: 64–74.
3 Querfurth HW, LaFerla FM. Alzheimer's disease. *N Engl J Med* 2010; **362**: 329–344.
4 Schrijvers EM, Witteman JC, Sijbrands EJ, Hofman A, Koudstaal PJ, Breteler MM. Insulin metabolism and the risk of Alzheimer disease: the Rotterdam Study. *Neurology* 2010; **75**: 1982–1987.
5 Whitmer RA, Karter AJ, Yaffe K, Quesenberry CP Jr, Selby JV. Hypoglycemic episodes and risk of dementia in older patients with type 2 diabetes mellitus. *JAMA* 2009; **301**: 1565–1572.
6 Rizzo MR, Marfella R, Barbieri M *et al.* Relationships between daily acute glucose fluctuations and cognitive performance among aged type 2 diabetic patients. *Diabetes Care* 2010; **33**: 2169–2174.
7 Wrighten SA, Piroli GG, Grillo CA, Reagan LP. A look inside the diabetic brain: contributors to diabetes-induced brain aging. *Biochim Biophys Acta* 2009; **1792**: 444–453.
8 Luchsinger JA. Diabetes, related conditions, and dementia. *J Neurol Sci* 2010; **299**: 35–38.
9 McClean PL, Parthsarathy V, Faivre E, Holscher C. The diabetes drug liraglutide prevents degenerative processes in a mouse model of Alzheimer's disease. *J Neurosci Nurs* 2011; **31**: 6587–6594.
10 Une K, Takei YA, Tomita N *et al.* Adiponectin in plasma and cerebrospinal fluid in MCI and Alzheimer's disease. *Eur J Neurol* 2011; **18**: 1006–1009.
11 Sims-Robinson C, Kim B, Rosko A, Feldman EL. How does diabetes accelerate Alzheimer disease pathology? *Nat Rev Neurol* 2010; **6**: 551–559.
12 Peila R, Rodriguez BL, Launer LJ. Type 2 diabetes, APOE gene, and the risk for dementia and related pathologies: the Honolulu-Asia Aging Study. *Diabetes* 2002; **51**: 1256–1262.
13 Beeri MS, Silverman JM, Davis KL *et al.* Type 2 diabetes is negatively associated with Alzheimer's disease neuropathology. *J Gerontol A Biol Sci Med Sci* 2005; **60**: 471–475.
14 Matsuzaki T, Sasaki K, Tanizaki Y *et al.* Insulin resistance is associated with the pathology of Alzheimer disease: the Hisayama study. *Neurology* 2010; **75**: 764–770.
15 Arvanitakis Z, Schneider JA, Wilson RS *et al.* Diabetes is related to cerebral infarction but not to AD pathology in older persons. *Neurology* 2006; **67**: 1960–1965.
16 Ahtiluoto S, Polvikoski T, Peltonen M *et al.* Diabetes, Alzheimer disease, and vascular dementia: a population-based neuropathologic study. *Neurology* 2010; **75**: 1195–1202.
17 Ott A, Stolk RP, van Harskamp F, Pols HA, Hofman A, Breteler MM. Diabetes mellitus and the risk of dementia: the Rotterdam Study. *Neurology* 1999; **53**: 1937–1942.
18 Beeri MS, Schmeidler J, Silverman JM *et al.* Insulin in combination with other diabetes medication is associated with less Alzheimer neuropathology. *Neurology* 2008; **71**: 750–757.
19 Longstreth WT Jr, Bernick C, Manolio TA, Bryan N, Jungreis CA, Price TR. Lacunar infarcts defined by magnetic

resonance imaging of 3660 elderly people: the Cardiovascular Health Study. *Arch Neurol* 1998; **55**: 1217–1225.

20 Vermeer SE, Den Heijer T, Koudstaal PJ, Oudkerk M, Hofman A, Breteler MM. Incidence and risk factors of silent brain infarcts in the population-based Rotterdam Scan Study. *Stroke* 2003; **34**: 392–396.

21 Araki Y, Nomura M, Tanaka H *et al*. MRI of the brain in diabetes mellitus. *Neuroradiology* 1994; **36**: 101–103.

22 den Heijer T, Vermeer SE, van Dijk EJ *et al*. Type 2 diabetes and atrophy of medial temporal lobe structures on brain MRI. *Diabetologia* 2003; **46**: 1604–1610.

23 Schmidt R, Launer LJ, Nilsson LG *et al*. Magnetic resonance imaging of the brain in diabetes: the Cardiovascular Determinants of Dementia (CASCADE) Study. *Diabetes* 2004; **53**: 687–692.

24 Minoshima S, Giordani B, Berent S, Frey KA, Foster NL, Kuhl DE. Metabolic reduction in the posterior cingulate cortex in very early Alzheimer's disease. *Ann Neurol* 1997; **42**: 85–94.

25 Mistur R, Mosconi L, Santi SD *et al*. Current Challenges for the Early Detection of Alzheimer's Disease: brain Imaging and CSF Studies. *J Clinl Neurol (Seoul, Korea)* 2009; **5**: 153–166.

26 Baker LD, Cross DJ, Minoshima S, Belongia D, Watson GS, Craft S. Insulin resistance and Alzheimer-like reductions in regional cerebral glucose metabolism for cognitively normal adults with prediabetes or early type 2 diabetes. *Arch Neurol* 2011; **68**: 51–57.

27 Furumoto S, Okamura N, Iwata R, Yanai K, Arai H, Kudo Y. Recent advances in the development of amyloid imaging agents. *Curr Top Med Chem* 2007; **7**: 1773–1789.

28 Kudo Y, Okamura N, Furumoto S *et al*. 2-(2-[2-Dimethylaminothiazol-5-yl]ethenyl)-6- (2-[fluoro]ethoxy) benzoxazole: a novel PET agent for in vivo detection of dense amyloid plaques in Alzheimer's disease patients. *J Nucl Med* 2007; **48**: 553–561.

29 Okamura N, Fodero-Tavoletti MT, Kudo Y *et al*. Advances in molecular imaging for the diagnosis of dementia. *Expert Opin Med Diagn* 2009; **3**: 705–716.

30 Arai H, Okamura N, Furukawa K, Kudo Y. Geriatric medicine, Japanese Alzheimer's disease neuroimaging initiative and biomarker development. *Tohoku J Exp Med* 2010; **221**: 87–95.

31 Furukawa K, Okamura N, Tashiro M *et al*. Amyloid PET in mild cognitive impairment and Alzheimer's disease with BF-227: comparison to FDG-PET. *J Neurol* 2010; **257**: 721–727.

32 McKhann G, Drachman D, Folstein M, Katzman R, Price D, Stadlan EM. Clinical diagnosis of Alzheimer's disease: report of the NINCDS-ADRDA Work Group under the auspices of Department of Health and Human Services Task Force on Alzheimer's Disease. *Neurology* 1984; **34**: 939–944.

33 Matsui T, Higuchi M, Okamura N, Arai H, Sasaki H. A practical method to predict rate of cognitive decline in mild to moderate Alzheimer's disease. *Neurology* 1999; **53**: 2208–2209.

34 Fazekas F, Kleinert R, Offenbacher H *et al*. Pathologic correlates of incidental MRI white matter signal hyperintensities. *Neurology* 1993; **43**: 1683–1689.

35 Zhao WQ, De Felice FG, Fernandez S *et al*. Amyloid beta oligomers induce impairment of neuronal insulin receptors. *FASEB J* 2008; **22**: 246–260.

Cholinergic Deficit and Response to Donepezil Therapy in Parkinson's Disease with Dementia

Kotaro Hiraoka[a]   Nobuyuki Okamura[c]   Yoshihito Funaki[b]   Akiko Hayashi[d]
Manabu Tashiro[a]   Kinya Hisanaga[f]   Toshikatsu Fujii[d]   Atsushi Takeda[e]
Kazuhiko Yanai[c]   Ren Iwata[c]   Etsuro Mori[d]

Divisions of [a]Cyclotron Nuclear Medicine and [b]Radiopharmaceutical Chemistry, Cyclotron and Radioisotope Center, Tohoku University, Departments of [c]Pharmacology, [d]Behavioral Neurology and Cognitive Neuroscience and [e]Neurology, Tohoku University Graduate School of Medicine, Sendai, and [f]Departments of Neurology and Clinical Research, Miyagi National Hospital, Watari, Japan

Abstract

Background: Although donepezil, an acetylcholinesterase inhibitor, has been proved to be effective in ameliorating cognitive impairment in Parkinson's disease with dementia (PDD), the responsiveness of patients to donepezil therapy varies. [5-^{11}C-methoxy]donepezil, the radiolabeled form of donepezil, is a ligand for positron emission tomography (PET), which can be exploited for the quantitative analysis of donepezil binding to acetylcholinesterase and for cholinergic imaging. **Objectives:** To investigate the deficits of the cholinergic system in the brain in PDD and its association with response to donepezil therapy. **Methods:** Twelve patients with PDD and 13 normal control subjects underwent [5-^{11}C-methoxy]donepezil-PET imaging. For patients with PDD, daily administration of donepezil was started after [5-^{11}C-methoxy]donepezil-PET imaging and continued for 3 months. **Results:** In the PDD group, the mean total distribution volume of the cerebral cortices was 22.7% lower than that of the normal control group. The mean total distribution volume of the patients with PDD was significantly correlated with improvement of visuoperceptual function after 3 months of donepezil therapy. **Conclusion:** The results suggest that donepezil therapy is more effective in patients with less decrease in acetylcholinesterase, a binding site of donepezil, at least in the specific cognitive domain.

Copyright © 2012 S. Karger AG, Basel

Introduction

Patients with Parkinson's disease (PD) often show cognitive deficits, including in the domains of memory, executive, visuoperceptual, and visuospatial functions, even early in the course of the disease [1]. Dementia is common among patients with PD, with a prevalence of 40% in cross-sectional studies [2] and a cumulative prevalence approaching 80% [3].

The cholinergic system is involved in the manifestation of cognitive impairment. The activities of choline acetyltransferase, the enzyme that synthesizes acetylcholine, and acetylcholinesterase, the enzyme that degrades acetylcholine, are decreased in the neocortex and hippocampus in PD with dementia (PDD) [4]. A significant loss of cholinergic neurons in the nucleus basalis of Meynert is noted in PDD [5]. Based on these findings, several acetylcholinesterase inhibitors, which potentiate cholinergic neurotransmission, are widely used to treat dementia.

[5-^{11}C-methoxy]donepezil ([^{11}C]donepezil), the radiolabeled form of the acetylcholinesterase inhibitor donepezil, is a ligand for positron emission tomography (PET), which measures donepezil binding to acetylcholinesterase to examine cholinergic function [6, 7]. A study involving [^{11}C]donepezil-PET that was carried out on patients with Alzheimer's disease (AD) showed significant reduction of donepezil binding in the brain in AD, compared with the normal elderly subjects [8].

Although donepezil has been proved to be effective in ameliorating cognitive impairment in PDD [9], the responsiveness of patients to donepezil therapy varies, for reasons that have not been clarified. We hypothesized that responsiveness to donepezil therapy has an association with the degree of cholinergic deficit in the brain. In this study, we investigated the deficits of the cholinergic system in PDD by quantifying acetylcholinesterase distribution, and the relationship between the deficits of the cholinergic system and clinical response to donepezil therapy.

Table 1. Demographic and clinical data of subjects studied with ^{11}C-donepezil PET

	PDD	Control	p value
n	12	13	
Sex (M:F)	9:3	10:3	NS[a]
Age, years	69.8 ± 6.4	69.5 ± 6.7	NS[b]
Education, years	12 ± 3.2	13.8 ± 2.7	NS[b]
MMSE (max. 30)	21.8 ± 4.2	29.8 ± 0.4	<0.000001[b]
UPDRS part III (max. 108)	23.1 ± 9.6		
Symptom duration, years			
Parkinsonism	11.3 ± 7.2		
Dementia	2 ± 1.6		

Antiparkinson medication	Number of treated patients	Dose range mg
Levodopa	12	300–700
Pramipexole	6	0.5–3
Cabergoline	3	2.0
Amantadine	2	150–200
Pergolide	3	0.5–0.75
Droxidopa	4	300–900
Entacapone	3	300–800
Selegiline	7	2.5–10
Risperidone	1	4.0
Quetiapine	4	25–150

Values are expressed as mean ± 1 SD.
[a] χ^2 test. [b] Two-tailed t test.
NS = Not significant (p > 0.05).

Materials and Methods

Subjects

Twelve patients with PDD and 13 healthy control subjects matched for age, sex, and education were enrolled in this study. The patients were selected from amongst those attending PD clinics at Miyagi National Hospital and Tohoku University Hospital. Board-certified neurologists made the diagnosis of PD according to the diagnostic criteria of the UK PD Society Brain Bank, based on clinical, laboratory, and radiological findings [10]. To select subjects with dementia, patients with a score of 1 or above in at least one of the sub-items of the Clinical Dementia Rating (CDR) [11] (even if overall CDR was 0.5) were included in this study. The exclusion criteria were a history of other neurological or psychiatric diseases, focal brain lesions, such as tumors and infarctions on magnetic resonance (MR) imaging, treatment with acetylcholinesterase inhibitors, anticholinergic drugs, or cholinergic drugs, and diagnostic criteria of dementia with Lewy bodies [12], i.e. development of the first signs of dementia before or within 1 year after the onset of motor symptoms.

The healthy control subjects were recruited from the local community through advertisements. Subjects with a history of neurological or psychiatric disease, a history suggestive of cognitive impairment, abnormal findings on neurological examination, ≤28 points on the Mini Mental-State Examination (MMSE) [13], abnormal findings on MR imaging, or medication with central nervous action were excluded.

Demographic data for the subjects are shown in table 1. The two groups did not show significant difference in terms of sex, age, and educational attainment. Mean score on the MMSE was significantly lower in the PDD group than in the control group. All patients received antiparkinsonian drugs. Four patients with PDD had been receiving antipsychotic drugs. Patients were clinically evaluated and scanned 'on' medication.

The Ethics Committee of Tohoku University School of Medicine approved the study protocol, and written informed consent was obtained from all healthy subjects and from patients with PDD or their family members when necessary.

Clinical Assessments and Donepezil Therapy

In the PDD patients, cognitive function and clinical symptoms were assessed by means of various cognitive tests in advance

of [11C]donepezil-PET imaging. The MMSE was used to assess general cognitive function. The Digit Span task in the Wechsler Adult Intelligence Scale-Revised (WAIS-R) [14] was used to evaluate attention. The Verbal Fluency task [15] and the Trail-Making Test-A (TMT-A) [15] were used to assess frontal lobe functions. Memory function was assessed by the Recall and Recognition task in the Japanese version of the Alzheimer's Disease Assessment Scale (ADAS) [16]. Visuoperceptual function was assessed by complex visual tasks, including object-size discrimination, form discrimination, overlapping figure identification, and visual counting tasks [17]. Neuropsychiatric symptoms were assessed by the modified version of the Neuropsychiatric Inventory (NPI) [18]. Motor dysfunction was assessed by the Unified Parkinson's Disease Rating Scale Part III (UPDRS Part III) [19].

After [11C]donepezil-PET imaging, donepezil therapy was initiated for all patients. Initially, patients were given donepezil 3 mg/day for 2 weeks and then the dose was increased to 5 mg/day, which is the standard dose given for AD in Japan, and continued for the next 3 months. Any drugs that the patients were already taking, such as antiparkinson drugs, were not changed during the 3 months of donepezil therapy, and they were not given any other additional drugs during the period. After the 3 months of donepezil therapy, the same evaluations were repeated.

Radiosynthesis of [11C]Donepezil and PET Procedures

Radiosynthesis of [11C]donepezil and PET procedures have been described previously [6, 7]. Briefly, tetrabutylammonium hydroxide was added to 5'-O-desmethylprecursor (M2) dissolved in methylethylketone. [11C]methyliodide was produced from [11C]CO_2 and then converted to [11C]methyl-triflate ([11C]MeOTf). [11C]donepezil was produced on the loop from [11C]MeOTf and purified in preparative high-performance liquid chromatography (HPLC). The obtained radioactivity of [11C]donepezil was 319.2 ± 149.0 MBq (mean ± SD), and the radiochemical yield was estimated to be 25–30% based on [11C]MeOTf after decay-correction. The specific activity of [11C]donepezil at the end of synthesis was 332.9 ± 115.0 GBq/μmol. Radiochemical purity was higher than 99%. The injected doses were 200 ± 118 MBq (5.4 ± 1.6 mCi). The PET scanner SET-2400W (Shimadzu Co., Kyoto, Japan) was used. The scanner acquires 63 image slices at a center-to-center interval of 3.125 mm and has a transaxial resolution of 3.9 mm full width at half maximum (FWHM), and an axial resolution of 4.5 FWHM at center of field of view [20]. Initially, 7-min transmission data were acquired with a rotating [68Ge]/[68Ga] line source for correcting attenuation. Then, after intravenous injection of [11C]donepezil, a 60-min dynamic scan in three-dimensional (3D) mode (30 s × 5 frames, 60 s × 5 frames, 150 s × 5 frames, 300 s × 8 frames) was performed. Subjects were scanned under standard resting conditions. During the scan, arterial blood samples (2.5 ml each) were collected from each patient's radial artery at 10-second intervals for the first 2 min, and subsequently at intervals increasing progressively from 1 to 10 min until 60 min after the injection of [11C]donepezil. 8 ml of additional blood was obtained at 5, 15 and 30 min for analysis of labeled metabolites. The plasma obtained by centrifugation was weighed and the radioactivity was measured. The metabolites of [11C]donepezil in the extra plasma samples were analyzed by HPLC. Briefly, sampled plasma (4 ml) was treated with 1 M $HClO_4$:MeCN (7:3) and centrifuged at 3,000 g for 3 min. The extracted supernatant solution was injected into a semipreparative HPLC column (YMC

ODS A-324, YMC Co. Ltd., Kyoto, Japan; 10 mm ID × 30 cm long) with a solvent system of 0.1 M ammonium formate:acetonitrile (60:40) at a flow rate of 5.0 ml/min. The eluates were collected at 30-sec intervals, and radioactivity was counted with a γ-counter. Metabolite correction was performed on pTAC using a previously described method [7]. Briefly, the empirical function for expressing the fraction of untransformed tracer remaining at time t, $1/(1+(\alpha t)^2)\beta$, was fitted with a Nelder-Meads simplex algorithm [21] using a least-squares method with initial guesses of 0.1 for both α and β. The acquired PET and metabolite-corrected blood data were analyzed using software PMOD (PMOD Technologies Ltd., Adliswil, Switzerland), which calculates quantitative parameters based on kinetic modeling. Parametric 3D maps of total distribution volume (tDV) in the brain were generated using the classical Logan plot [22] as implemented in PMOD software.

PET Image Analysis

Images were analysed using software SPM8 (Wellcome Department of Cognitive Neurology, London, UK [http://www.fil.ion.ucl.ac.uk/spm/software/spm8/]) and ImageJ 1.42q (National Institutes of Health, Bethesda, Md., USA [http://rsb.info.nih.gov/ij/]), based on built-in functions.

Region of Interest Analysis

The tDVs of the total cerebral cortices were calculated using a semi-automatic method. Axial, three-dimensional spoiled gradient echo images or magnetization-prepared rapid gradient echo images were obtained from a 1.5-T MRI unit (Signa Horizon LX CV/i; GE Healthcare, Milwaukee, Wisc., USA, or Magnetom Symphony; Siemens, Tokyo, Japan) for anatomical reference, which were segmented into gray and white matter using the SPM8 prior probability templates. The intensity nonuniformity bias, which is caused by a smooth, spatially varying artifact induced by the scanner, was corrected to aid segmentation. The total cerebral cortices in the probability maps of the gray matter were extracted by tracing with a manually driven mouse cursor on ImageJ with threshold of the probability maps set at 0.5. They were co-registered to the tDV images of each subject. The co-registered images were used as mask images of the cerebral cortices, and were projected to tDV images of each subject to extract the cerebral cortices on the tDV images. Finally, the mean tDV value of the cerebral cortices was calculated using the histogram function of ImageJ.

The two-tailed t test was used for group comparison. Spearman's simple correlation and then partial correlations covarying out the effects of sex, age and education were used for correlation analysis between mean tDVs of the cerebral cortices and the results of the cognitive tests at baseline and the cognitive improvements after 3 months of donepezil therapy. The software SPSS 17.0 (SPSS Inc., Chicago, Ill., USA) was used for the statistical analysis. The statistical significance level was set at $p < 0.05$. The significance level for multiple comparisons was not corrected because of the explorative nature of this study.

Statistical Parametric Mapping (SPM) Analysis

The template image of tDV was created using the 3D gradient-echo MR images in the 13 healthy control subjects. Using SPM8, the MR images were coregistered to tDV image, and both MR and tDV images were spatially normalized to a standard anatomic orientation (Montreal Neurological Institute space) by obtaining parameters from MR images. Then, the template tDV image was

Table 2. Results of clinical assessments before and after 3 months of oral administration of donepezil in patients with Parkinson's disease dementia (n = 12)

	Score range	Pre-treatment	Post-treatment	p value*
MMSE	0–30	21.8±4.2	23.0±3.4	0.187
Digit span (WAIS-R)	0–28	8.1±3.1	7.8±3.0	0.536
Fluency				
Phonetic	–	11.6±4.3	13.0±6.3	0.402
Animals	–	8.3±3.3	8.9±3.4	0.457
TMT-A	–	162.8±81.8	166.7±110.7	0.896
Recall test (ADAS)	0–10	5.6±1.7	5.6±1.4	1.000
Recognition test (ADAS)	0–12	3.3±2.6	3.9±3.3	0.549
Visuoperceptual test	0–90	76.6±23.5	83.4±5.8	0.320
NPI	0–144	13.2±11.9	7.3±7.7	0.058
UPDRS part III	0–108	23.1±9.6	22.7±12.1	0.798

Values are expressed as mean ± 1 SD.
* Paired t test.
NS = Not significant (p > 0.05).
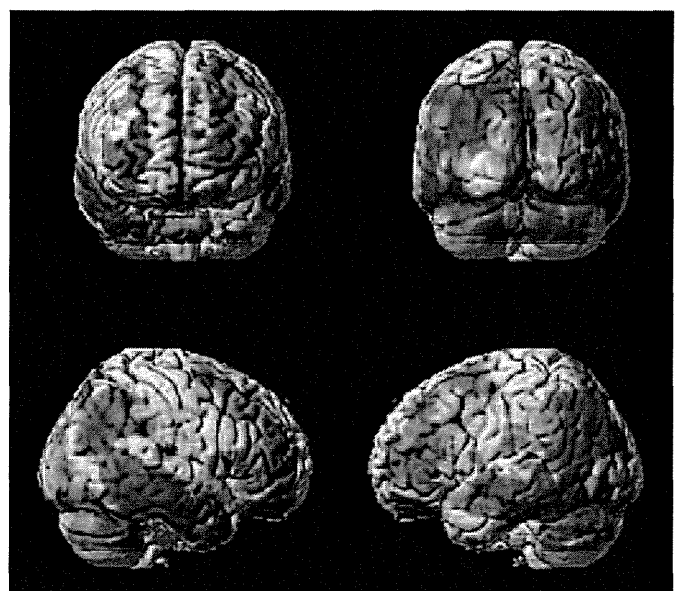
Fig. 1. Regions with significant [^{11}C]donepezil tDV decrease in the group of PDD as compared with the normal control group. Coronal (upper row) and sagittal (lower row) views in projection onto a standard MRI as 3D surface projection (SPM8, $p_{uncorrected} <$ 0.005, cluster extent threshold 100 voxels).

generated by averaging these 13 normalized images and smoothing the averaged images using an 8-mm Gaussian kernel, as 8-mm smoothing is used for the estimation of normalization parameters in SPM8. Parametric tDV images were normalized using the tDV template and written using bilinear interpolation. Finally, a Gaussian kernel of 8 mm was used in smoothing of the parametric images. As tDV is an absolute value, SPM analysis was performed without global normalization. The between-group comparison that examines the difference in tDV values at voxel level was performed using analysis of covariance (ANCOVA) with sex, age, and education as covariates as an explorative analysis covering the whole brain without any a-priori hypothesis.

Correlation analyses between tDV and cognitive assessments at baseline, and between tDV and cognitive improvements after 3 months of donepezil therapy in PDD patients were also performed for each voxel with and without covarying out the effects of sex, age, and education and using the general linear approach. Statistical significance level was set at p < 0.005 without correction for multiple comparison and cluster extent threshold was 100 voxels.

Results

The results of cognitive and clinical assessments at baseline and after 3 months of donepezil therapy for patients with PDD are shown in table 2. The MMSE, verbal fluency, complex visual tasks, and NPI showed an improvement; however, the changes did not reach statistical significance. The mean tDVs of the cerebral cortices in

the PDD group (7.9 ± 2.2 ml/ml) were significantly lower than those of the control group (10.2 ± 2.7 ml/ml) in the mean decrease rate of 22.7% (p = 0.028). In the SPM analysis, the PDD group exhibited a widespread tDV reduction as compared with the control group, comprising nearly the entire brain (fig. 1).

In the Spearman's simple correlation analysis, mean tDVs of the cerebral cortices did not show significant correlation with cognitive improvements after 3 months of donepezil therapy. In the partial correlation analyses (table 3), the improvement of the visuoperceptual test score showed significant positive correlation with tDVs of the cerebral cortices (correlation coefficient = 0.837, p = 0.005). SPM correlation analysis without covarying out the effects of sex, age and education did not show significant correlation between tDVs and the cognitive improvements after 3 months of donepezil therapy. SPM correlation analysis with covarying out the effects of sex, age and education did not show a localized correlated region in the brain, but showed diffuse positive correlation between tDVs and change in visuoperceptual test after 3 months of donepezil therapy. Neither region of interest analysis (table 3) nor SPM analysis showed significant correlation between the cognitive assessments at baseline and tDV.

Table 3. Correlation matrix contrasting mean tDV of the cerebral cortices against the results of cognitive tests at baseline and change in the cognitive tests after 3 months of donepezil therapy

	MMSE	Digit span (WAIS-R)	Fluency	TMT-A	Recall task (ADAS)	Recognition task (ADAS)	Visuoper-ceptual test	NPI
Baseline								
Correlation coefficient	0.185	−0.457	−0.618	0.030	0.223	−0.621	−0.402	0.147
p	0.634	0.216	0.076	0.954	0.564	0.075	0.283	0.705
Change								
Correlation coefficient	−0.207	−0.036	0.165	0.116	−0.406	0.207	0.837	−0.091
p	0.593	0.928	0.672	0.827	0.278	0.594	0.005	0.817

Discussion

Our study showed that acetylcholinesterase in the cerebral cortices decreased in PDD. The density of acetylcholinesterase in the cerebral cortices of patients with PDD significantly correlated with improvements in visuoperceptual function after 3 months of donepezil therapy.

There are previous studies of cholinergic PET imaging utilizing radiolabeled acetylcholine analogues, such as N-[^{11}C]methyl-piperidin-4-yl propionate ([^{11}C]PMP). In the studies of Hilker et al. [23] and Bohnen et al. [24] using [^{11}C]PMP, PD with dementia showed 20.0–29.7% reduction of cortical acetylcholinesterase activity and PD without dementia showed 10.7–12.9% reduction of cortical acetylcholinesterase activity compared with normal subjects. It is possible that the results using [^{11}C]donepezil-PET may differ from those of PET imaging studies using radiolabeled acetylcholine analogues because [^{11}C]donepezil-PET may have an advantage in that it directly measures the density of acetylcholinesterase in the brain tissue regardless of acetylcholinesterase activity, whereas PET imaging using radiolabeled acetylcholine analogues measures acetylcholinesterase activity as the acetylcholine analogues are catabolized by acetylcholinesterase and then trapped in the brain tissue. However, the reduction rate of the mean tDV value of the cerebral cortices in the PDD group was similar to that of cortical acetylcholinesterase activity in the previous studies [23, 24]. SPM analysis in this study revealed a global reduction of acetylcholinesterase density in the brains of PDD patients, which was also similar to the results of previous studies [23, 25].

In the study involving the use of [^{11}C]donepezil-PET on patients with AD [8], patients with mild AD (n = 5, mean MMSE = 25.0) exhibited an approximately 18–20%

reduction of donepezil binding in the neocortex and hippocampus, and patients with modererate AD (n = 5, mean MMSE = 15.4) exhibited an approximately 24–30% reduction of donepezil binding throughout the brain compared with the normal controls. The PDD patients in our study showed reduction rates in line with those of AD patients in the previous study [8] in the light of dementia severity, although previous pathological and cholinergic imaging studies [24, 26] showed that cortical cholinergic function is more severely affected in PDD than in AD. This may be due to the fact that the mean age of the subjects was not sufficiently matched between the groups in the AD study [8].

The mean tDVs of the cerebral cortices significantly correlated with changes in visuoperceptual test score after 3 months of donepezil therapy, which indicated that more improvement in visuoperceptual functions was observed in the patients with relatively higher density of acetylcholinesterase in the cerebral cortices. As the correlation was overshadowed by covariates, partial correlation analysis revealed the correlation, whereas simple correlation analysis did not. This would probably make it difficult to identify responders prospectively using PET in clinical situations. However, donepezil-PET is useful in research into pharmacokinetics of donepezil, condition of the cholinergic system in the brains of dementia patients, and their association with the therapeutic effect on dementia patients. Density of acetylcholinesterase, which is localized predominantly in cholinergic cell bodies and axons [27] and may be downregulated as a compensatory action in the face of cholinergic degeneration, was measured as a marker of cholinergic function. However, a proportional relationship between acetylcholinesterase density and cholinergic function is unproven, and it is possible that some patients have the same degree of cholinergic degeneration but relatively higher acetylcho-

linesterase density and further acetylcholine reduction than others. In patients with relatively higher density of acetylcholinesterase, donepezil therapy may be more effective because there are more binding sites for donepezil. The specific correlation between cortical tDVs and improvement of visuoperceptual function after donepezil therapy indicates that visuoperceptual deficit has profound relevance to cortical cholinergic deficits, which is in accordance with some researchers' suggestion that cortical cholinergic deficits underlie the temporoposterior type of cognitive phenotype, while dysexecutive syndrome is mediated mainly by fronto-striatal dopaminergic dysfunction in PD [1, 28]. Although it seems that visuoperceptual deficit, one of the core features of cognitive dysfunction in PD [1, 29], may have deteriorating effects on activities of daily living ability in PDD patients, whether or not the improvements in the subgroup of PDD patients with high donepezil binding actually make a clinical difference is unknown, as we evaluated global clinical status only at baseline using the CDR and did not evaluate changes in global clinical status after donepezil therapy.

There are some limitations to this study. The first is that [^{11}C]donepezil-PET was performed without washing out daily medications, including antiparkinson drugs, which might affect the results of [^{11}C]donepezil-PET. The second limitation is that the significance level in statistical analyses was not corrected for multiple comparisons because of the exploratory nature of the study. Finally, unlike the previous study [30], the association between the inhibition ratio of acetylcholinesterase by donepezil and its therapeutic effect was not determined in this study as we did not perform [^{11}C]donepezil-PET after the donepezil therapy.

In conclusion, the results of this study suggest that density of acetylcholinesterase is decreased in PDD and that donepezil is more effective in patients with less decrease of acetylcholinesterase, a binding site of donepezil, at least in the specific cognitive domain.

References

1 Aarsland D, Bronnick K, Fladby T: Mild cognitive impairment in Parkinson's disease. Curr Neurol Neurosci Rep 2011;11:371–378.
2 Cummings J: Intellectual impairment in Parkinson's disease: clinical, pathologic, and biochemical correlates. J Geriatr Psychiatry Neurol 1988;1:24–36.
3 Aarsland D, Andersen K, Larsen JP, Lolk A, Kragh-Sorensen P: Prevalence and characteristics of dementia in Parkinson disease: an 8-year prospective study. Arch Neurol 2003; 60:387–392.
4 Perry EK, Curtis M, Dick DJ, Candy JM, Atack JR, Bloxham CA, Blessed G, Fairbairn A, Tomlinson BE, Perry RH: Cholinergic correlates of cognitive impairment in Parkinson's disease: comparisons with Alzheimer's disease. J Neurol Neurosurg Psychiatry 1985;48:413–421.
5 Whitehouse P, Hedreen J, White Cr, Price D: Basal forebrain neurons in the dementia of Parkinson disease. Ann Neurol 1983;13: 243–248.

6 Funaki Y, Kato M, Iwata R, Sakurai E, Tashiro M, Ido T, Yanai K: Evaluation of the binding characteristics of [5-(11)C-methoxy] donepezil in the rat brain for in vivo visualization of acetylcholinesterase. J Pharmacol Sci 2003;91:105–112.
7 Hiraoka K, Okamura N, Funaki Y, Watanuki S, Tashiro M, Kato M, Hayashi A, Hosokai Y, Yamasaki H, Fujii T, Mori E, Yanai K, Watabe H: Quantitative analysis of donepezil binding to acetylcholinesterase using positron emission tomography and [5-(11)C-methoxy]donepezil. Neuroimage 2009;46:616–623.
8 Okamura N, Funaki Y, Tashiro M, Kato M, Ishikawa Y, Maruyama M, Ishikawa H, Meguro K, Iwata R, Yanai K: In vivo visualization of donepezil binding in the brain of patients with Alzheimer's disease. Br J Clin Pharmacol 2008;65:472–479.
9 van Laar T, De Deyn P, Aarsland D, Barone P, Galvin J: Effects of cholinesterase inhibitors in Parkinson's disease dementia: a review of clinical data. CNS Neurosci Ther 2011;17:428–441.

10 Daniel S, Lees A: Parkinson's Disease Society Brain Bank, London: overview and research. J Neural Transm Suppl 1993;39:165–172.
11 Morris J: Clinical dementia rating: a reliable and valid diagnostic and staging measure for dementia of the Alzheimer type. Int Psychogeriatr 1997;9(suppl 1):173–176.
12 McKeith IG, Dickson DW, Lowe J, et al: Diagnosis and management of dementia with Lewy bodies: third report of the DLB Consortium. Neurology 2005;65:1863–1872.
13 Folstein MF, Folstein SE, McHugh PR: 'Mini-mental state'. A practical method for grading the cognitive state of patients for the clinician. J Psychiatr Res 1975;12:189–198.
14 Shinagawa F, Kobayashi S, Fujita K, Maekawa H: Japanese Wechsler Adult Intelligence Scale-Revised. Tokyo, Nihon Bunka Kagakusha, 1990.
15 Abe M, Suzuki K, Okada K, Miura R, Fujii T, Etsurou M, Yamadori A: Normative data on tests for frontal lobe functions: Trail Making Test, Verbal Fluency, Wisconsin Card Sorting Test (Keio version). No To Shinkei 2004; 56:567–574.

16 Mohs R, Rosen W, Davis K: The Alzheimer's Disease Assessment Scale: an instrument for assessing treatment efficacy. Psychopharmacol Bull 1983;19:448–450.

17 Mori E, Shimomura T, Fujimori M, Hirono N, Imamura T, Hashimoto M, Tanimukai S, Kazui H, Hanihara T: Visuoperceptual impairment in dementia with Lewy bodies. Arch Neurol 2000;57:489–493.

18 Mori S, Mori E, Iseki E, Kosaka K: Efficacy and safety of donepezil in patients with dementia with Lewy bodies: preliminary findings from an open-label study. Psychiatry Clin Neurosci 2006;60:190–195.

19 Fahn S, Elton R: Unified Parkinson's Disease Rating Scale; in Fahn S, Marsden C, Calne D, Goldstein M (eds): Recent Developments in PD. Florham Park, Macmillan Healthcare Information, 1987, pp 153–63.

20 Fujiwara T, Watanuki S, Yamamoto S, Miyake M, Seo S, Itoh M, Ishii K, Orihara H, Fukuda H, Satoh T, Kitamura K, Tanaka K, Takahashi S: Performance evaluation of a large axial field-of-view PET scanner: SET-2400W. Ann Nucl Med 1997;11:307–313.

21 Nelder JA, Mead R: A simplex-method for function minimization. Comput J 1965;7:308–313.

22 Logan J: Graphical analysis of PET data applied to reversible and irreversible tracers. Nucl Med Biol 2000;27:661–670.

23 Hilker R, Thomas A, Klein J, Weisenbach S, Kalbe E, Burghaus L, Jacobs AH, Herholz K, Heiss WD: Dementia in Parkinson disease: functional imaging of cholinergic and dopaminergic pathways. Neurology 2005;65:1716–1722.

24 Bohnen N, Kaufer D, Ivanco L, Lopresti B, Koeppe R, Davis J, Mathis CA, Moore RY, DeKosky ST: Cortical cholinergic function is more severely affected in parkinsonian dementia than in Alzheimer disease: an in vivo positron emission tomographic study. Arch Neurol 2003;60:1745–1748.

25 Shimada H, Hirano S, Shinotoh H, Aotsuka A, Sato K, Tanaka N, Ota T, Asahina M, Fukushi K, Kuwabara S, Hattori T, Suhara T, Irie T: Mapping of brain acetylcholinesterase alterations in Lewy body disease by PET. Neurology 2009;73:273–278.

26 Tiraboschi P, Hansen LA, Alford M, Merdes A, Masliah E, Thal LJ, Corey-Bloom J: Early and widespread cholinergic losses differentiate dementia with Lewy bodies from Alzheimer disease. Arch Gen Psychiatry 2002;59:946–951.

27 Wevers A: Localisation of pre- and postsynaptic cholinergic markers in the human brain. Behav Brain Res 2011;221:341–355.

28 Kehagia AA, Barker RA, Robbins TW: Neuropsychological and clinical heterogeneity of cognitive impairment and dementia in patients with Parkinson's disease. Lancet Neurol 2010;9:1200–1213.

29 Mosimann UP, Mather G, Wesnes KA, O'Brien JT, Burn DJ, McKeith IG: Visual perception in Parkinson disease dementia and dementia with Lewy bodies. Neurology 2004;63:2091–2096.

30 Bohnen NI, Kaufer DI, Hendrickson R, Ivanco LS, Lopresti BJ, Koeppe RA, Meltzer CC, Constantine G, Davis JG, Mathis CA, Dekosky ST, Moore RY: Degree of inhibition of cortical acetylcholinesterase activity and cognitive effects by donepezil treatment in Alzheimer's disease. J Neurol Neurosurg Psychiatry 2005;76:315–319.

Studies on electrooxidation of lignin and lignin model compounds. Part 1: Direct electrooxidation of non-phenolic lignin model compounds

Takumi Shiraishi[1,*], Toshiyuki Takano[1], Hiroshi Kamitakahara[1] and Fumiaki Nakatsubo[1,2]

[1] Division of Forest and Biomaterials Science, Graduate School of Agriculture, Kyoto University, Kyoto, Japan

[2] Research Institute for Sustainable Humanosphere, Kyoto University, Kyoto, Japan

*Corresponding author.
Division of Forest and Biomaterials Science, Graduate School of Agriculture, Kyoto University, Sakyo-ku Kyoto, 606-8502, Japan
Phone: +81-75-753-6256
Fax: +81-75-753-6300
E-mail: tkulash@kais.kyoto-u.ac.jp

Abstract

The direct anodic oxidation of non-phenolic lignin model compounds was investigated to understand their basic behaviors. The results of cyclic voltammetry (CV) studies of monomeric model, such as 1-(4-ethoxy-3-methoxyphenyl)ethanol, are interpreted as the oxidation for C_α-carbonylation did not proceed in the reaction without a catalyst, but a base promotes this reaction. Indeed, the bulk electrolyses of the monomeric lignin model compounds with 2,6-lutidine afforded the corresponding C_α-carbonyl compounds in high yields (60–80%). It is suggested that deprotonation at C_α-H in the ECEC mechanism (E=electron transfer and C=chemical step) is important for C_α-carbonylation. In the uncatalyzed bulk electrolysis of a β-O-4 model dimeric compound, 4-ethoxy-3-methoxyphenylglycerol-β-guaiacyl ether, the corresponding C_α-carbonyl compound was not detected but as a result of C_α-C_β cleavage 4-O-ethylvanillin was found in 40% yield. In the electrolysis reaction in the presence of 2,6-lutidine (as a sterically hindered light base), the reaction stopped for a short time unexpectedly. These results indicate the different electrochemical behavior of simple monomeric model compounds and dimeric β-O-4 models. The conclusion is that direct electrooxidation is unsuitable for C_α-carbonylation of lignin.

Keywords: C_α-carbonylation; cyclic voltammetry (CV); direct electrooxidation; ECEC mechanism; lignin.

Introduction

The kraft pulping process is known to proceed via initial, bulk, and final delignification phases (Sjöblom 1996). The main delignification occurs during the bulk phase, but its drastic conditions cause appreciable degradation of carbo-

hydrates. Therefore, a pretreatment to facilitate the delignification in the bulk phase would be desirable for high-yield pulping. The rate-determining step in the bulk delignification is thought to be cleavage of non-phenolic β-O-4 linkages (Ljunggren 1980). On the other hand, it has been reported that the alkali cleavage of non-phenolic β-O-4 linkages is significantly accelerated by the presence of α-carbonyl groups (Gierer and Ljunggren 1979; Gierer et al. 1980). The positive effect of α-carbonyl groups has been also found in alkaline hydrogen peroxide bleaching and oxygen alkaline cooking (Aoyagi et al. 1980; Hosoya and Nakano 1980). Accordingly, the introduction of α-carbonyl groups into non-phenolic β-O-4 substructure is one of the targets of a pretreatment for kraft pulping. In this context, pretreatment with 2,3-dichloro-5,6-dicyano-1,4-benzoquinone (DDQ) (Gierer and Norén 1982) and pyridium dichromate (PDC) (Ljunggren and Olsson 1984) was reported. Electrooxidation (anodic oxidation) could be an environmentally friendly method to introduce α-carbonyl groups (C_α-carbonylation) in lignin, which could avoid the utilization of expensive and/or hazardous reagents.

However, it is well known that C_α-C_β cleavage (leading to aldehyde formation) often takes place simultaneously as a result of oxidation of β-O-4 linkages (Baciocchi et al. 2000). The reaction is also important for the formation of phenolic substructures which are degraded in the initial phase under milder conditions in the case of high-yield pulping and yield vanillin. The electrooxidation of lignin for the production of vanillin was also reported (Smith et al. 1989; Lalvani and Rajagopal 1993; Parpot et al. 2000). But even in this case, the cleavage of non-phenolic β-O-4 substructure is a key reaction. There are a few reports concerning electrooxidation of lignin in alkali medium (Limosin et al. 1986; Löbbecke et al. 1990) for non-energetic lignin utilization, but they did not discuss C_α-carbonylation. Many fundamental studies on electrochemical oxidation were performed with lignin model compounds (Steelink and Britton 1974; Britton and Steelink 1974; Chabaud and Sundholm 1978; Sundholm 1982; Limosin and Canquis 1985; Pardini et al. 1991, 1992). However, these papers were dealing mainly with phenolic model compounds; the aspects of non-phenolic compounds were neglected.

The present study focuses on the electrooxidation of lignin and lignin model compounds, mainly from the point of view of C_α-carbonylation as a pretreatment for kraft pulping. The direct electrooxidation of non-phenolic lignin model compounds without a mediator will be described to understand the basics of this type of reaction.
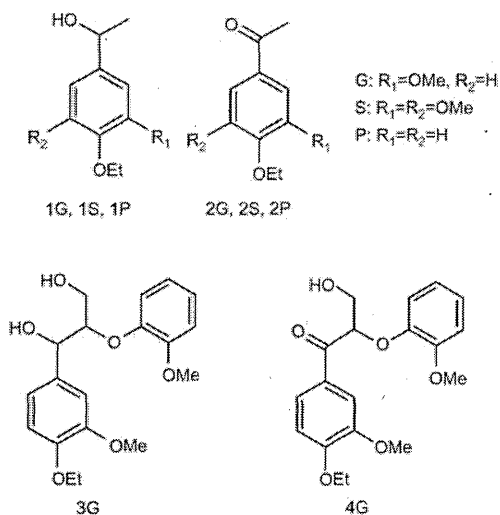
Figure 1 Non-phenolic lignin model compounds investigated in the present study.

Materials and methods

Materials

For substance abbreviations see Figure 1. Non-phenolic monomeric lignin model compounds [1-(4-ethoxy-3-methoxyphenyl)ethanol (1G), 1-(4-ethoxy-3,5-dimethoxyphenyl)ethanol (1S), and 1-(4-ethoxyphenyl)ethanol (1P)] were prepared from acetovanillone, 4-hydroxy-3,5-dimethoxyacetophenone, and 4-hydroxyacetophenone by conventional ethylation: [EtI/K_2CO_3/N,N-dimethyl formamide (DMF)/room temperature (r.t.) for 2G and 2P, or 40°C for 2S/6 h] and reduction (NaBH$_4$/MeOH/r.t./0.3 h), respectively. The non-phenolic dimeric lignin model compound (4-ethoxy-3-methoxyphenyl-glycerol-β-guaiacyl ether, 3G) was prepared from 4-hydroxy-3-methoxyphenylglycerol-β-guaiacyl ether (Nakatsubo et al. 1975) by conventional ethylation (EtI/K_2CO_3/acetone/reflux/6 h). 1-(4-Ethoxy-3-methoxyphenyl)-3-hydroxy-2-(2-methoxyphenoxy)-1-propanone (4G) was prepared from 2G (Crestini and D'Auria 1997).

Other chemicals were purchased from Nacalai Tesque Inc. (Kyoto, Japan) and used as received.

Methods

Cyclic voltammetry Cyclic voltammetry (CV) measurements were run in an undivided cell (5 ml) using a 1.6 mm diameter platinum disk-working electrode by an ALS electrochemical analyzer (ALS 650B). The reference electrode was Ag/Ag$^+$ (0.1 M LiClO$_4$, 0.01 M AgNO$_3$ in CH$_3$CN) and counter electrode was platinum wire. The electrolyte was 0.1 M LiClO$_4$/CH$_3$CN, and the substrate concentration was 5 mM.

Bulk electrolysis of non-phenolic monomers (1G, 1S, or 1P) The instrument for electrochemical oxidation was a divided cell equipped with a 2.4×3.0 cm^2 carbon felt electrode and an Ag/Ag$^+$ reference electrode (0.1 M LiClO$_4$, 0.01 M AgNO$_3$ in CH$_3$CN) in the anode chamber and a platinum wire electrode in the cathode chamber. The anode chamber was filled with 0.1 M LiClO$_4$ in CH$_3$CN (20 ml) and the cathode chamber with 0.1 M tetra-n-butyl ammonium perchlorate (TBAP) in CH$_3$CN (5 ml). The model compound was added to the anode chamber. Electrolysis was carried out under stirring at a fixed potential (in Table 1) by the ALS electrochemical analyzer equipped with a power booster (ALS 680) until the current dropped to about 1 mA. After electrolysis, CH$_3$CN (0.5 ml) containing 36 μmol benzhydrol was added to the anode chamber as an internal standard. The anolyte was extracted with EtOAc, and the organic layers were washed with distilled water, dried over Na$_2$SO$_4$, and concentrated to give colorless oil.

The product was dissolved in acetone and subjected to gas chromatography. A Shimadzu GC-18A system with a flame ionization detector (FID) was used. Conditions: fused silica capillary column (OV-17, 25 m×0.25 mm i.d., coated with 0.25 μm 50% phenyl-methylpolysiloxane, Shimadzu, Kyoto, Japan); temperature program: 150°C (10 min)→10°C min^{-1}→180°C (10 min)→10°C min^{-1}→230°C (10 min); injector temperature 270°C; detector temperature 270°C; carrier gas He (0.1 MPa).

Bulk electrolysis of a non-phenolic dimer (3G) The instrument was the same as indicated above. The anode chamber was filled with 0.1 M LiClO$_4$ in CH$_3$CN (20 ml) and the cathode chamber was filled with 0.1 M TBAP in CH$_3$CN (5 ml). Compound 3G was

Table 1 Bulk electrolyses of 1-(4'-ethoxyphenyl) ethanols (1G, 1S, 1P).

Entry	Substrate	Potential (V vs. Ag/Ag$^+$)	Catalyst	(eq)	Product	Yield[a] (%)	Electricity (Fmol^{-1})	Efficiency (%)
1	1G	1.0	2,6-Lutidine	3	2G	57.1	1.66	68.8
2	1G	1.0	2,6-Lutidine	5	2G	69.2	1.91	72.4
3	1G	1.0	2,6-Lutidine	10	2G	74.1	1.89	78.6
4	1G	1.0	2,6-Lutidine	20	2G	79.1	1.92	82.2
5	1G	1.0	2,6-Lutidine	30	2G	78.6	1.83	85.8
6	1G	1.0	—	—	2G	Trace	1.43	—
7	1S	1.0	2.6-Lutidine	5	2S	43.1	2.01	43.1
8	1S	1.0	2.6-Lutidine	10	2S	56.4	2.00	56.4
9	1S	1.0	2.6-Lutidine	20	2S	61.7	1.93	63.9
10	1P	1.4	2.6-Lutidine	5	2P	58.4	2.00	58.4
11	1P	1.4	2.6-Lutidine	10	2P	61.7	2.19	56.5
12	1P	1.4	2.6-Lutidine	20	2P	75.3	2.37	63.4
13	1G	1.0	Pyridine	20	2G	69.0	1.90	72.6
14	1G	1.0	2,4,6-Collidine	20	2G	91.0	1.93	94.0

[a]Yields were evaluated by GC using benzhydrol as an internal standard.

added to the anode chamber. Electrolysis was carried out under stirring at 1.1 V vs. Ag/Ag$^+$ by the ALS electrochemical analyzer equipped with the power booster (ALS 680) until the current dropped to about 1 mA. The anolyte was extracted with EtOAc, and the organic layers were washed with distilled water, dried over Na$_2$SO$_4$, and evaporated. The products were purified on a silica gel plate (Kisegel 60 F$_{254}$, Merck; 2 mm×20 cm×20 cm), the fraction (Rf=ca. 0.80; EtOAc/n-hexane 1:1) was isolated and subjected to nuclear magnetic resonance (NMR) spectroscopy (Varian INOVA 300 FT-NMR, 300 MHz, spectrometer); the solvent was CDCl$_3$ with TMS as an internal standard.

4-O-Ethylvanillin ^{1}H-NMR (CDCl$_3$): δ 1.52 (3H, t, J=6.9, -O-CH$_2$-C$\underline{H_3}$), 3.94 (3H, s, OCH$_3$), 4.20 (2H, q, J=6.9, -O-C$\underline{H_2}$-CH$_3$), 6.97 (1H, d, J=8.4, Arom-C$_5$-H), 7.42 (1H, d, J=2.1, Arom-C$_2$-H), 7.45 (1H, dd, J=8.4 and 2.1, Arom-C$_6$-H), 9.85 (1H, s, CHO).

Instrument for monitoring experiments: a divided cell equipped with a 1.0×1.0 cm^2 platinum plate electrode and an Ag/Ag$^+$ reference electrode (0.1 M LiClO$_4$, 0.01 M AgNO$_3$ in CH$_3$CN) in the anode chamber and a 1.0×1.0 cm^2 platinum plate electrode in the cathode chamber. The reaction mixture (50 μl) was sequentially sampled, diluted with 450 μl of water/CH$_3$CN (8:1, v/v) and subjected to high-performance liquid chromatography (HPLC) (Shimadzu LC-20AT LC system equipped with a photodiode array detector, SPD-M20A). Conditions: Cosmosil column 5C18MS (4.6×250 mm, Nacalai Tesque Inc., Kyoto, Japan); eluent water/CH$_3$CN (80/20, v/v); flow rate 1.0 ml min^{-1}; column oven temperature 40°C; detection at 280 nm.

Results and discussion

Electrooxidation of non-phenolic monomers

Before the bulk electrolyses of the monomers 1G, 1S, and 1P at a constant potential, cyclic voltammetry measurements were carried out to determine the oxidation potential. Figure 2(A) shows the cyclic voltammogram (CV) of compound 1G, and Figure 2(B) the corresponding α-carbonyl compound 2G in 0.1 M LiClO$_4$/CH$_3$CN without catalyst. In the former, the first oxidation peak (a) at 1.1 V was found, but a second peak, corresponding to the oxidation peak (b) of compound 2G at 1.3 V, was not clearly observed. Accordingly, compound 2G was not formed in the system.

Then, CV measurement of compound 1G in 0.1 M LiClO$_4$/CH$_3$CN with trifluoroacetic anhydride (TFA) was performed to understand the CV of compound 1G without catalyst, because it has been reported that addition of TFA was effective to detect unstable radical cation or dication intermediates in CV (Hammerich and Parker 1973). In the CV of compound 1G (Figure 3E), oxidation peaks (c) at 1.2 V and (d) at 1.8 V are visible. These correspond to the potentials of single-electron oxidation of compound 1G to radical cation 1Ga on the one hand, and to single-electron oxidation of compound 1Ga to dication 1Ga+, on the other hand (Figure 6a). A reduction peak (c′) at 1.1 V by reduction of radical cation 1Ga to 1G was also found in CV of compound 1G in the range of 0.9–1.6 V (Figure 3F). The oxidation peak (a) in the CV in the system without a catalyst is due to single-electron oxidation of compound 1G to radical cation 1Ga. On the other hand, the current of peak (a) in the
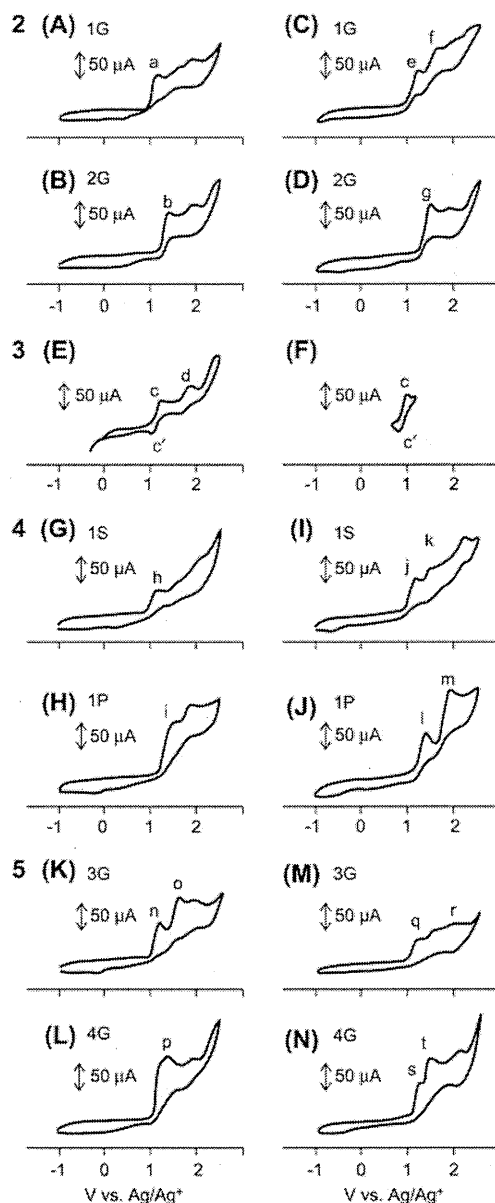
Figures 2–5 Cyclic voltammograms of the compounds presented in Figure 1. If not otherwise indicated, the reaction conditions were: in 0.1 M LiClO$_4$/CH$_3$CN; scan rate 0.1 Vs^{-1}. **(2)** Compounds 1G, 2G, without (A, B) and with 2,6-lutidine (C, D). **(3)** Compound 1G in TFA in 0.1 M LiClO$_4$/CH$_3$CN; scan rate 0.1 Vs^{-1}. **(4)** Compounds 1S, 1P, without (G, H) and with 2,6-lutidine (I, J). **(5)** Compounds 3G and 4G without (K, L) and with 2,6-lutidine (M, N).

CV in the system without a catalyst was almost twice as high as peak (c) in the CV in the system with TFA; probably, a single-electron was further withdrawn at 1.1 V in the system without a catalyst. However, it is difficult to withdraw a second electron from a radical cation (Sawyer et al. 1995). The oxidation potential of radical cation 1Ga to dication 1Ga+ was 1.8 V, as described above. It is supposed from these
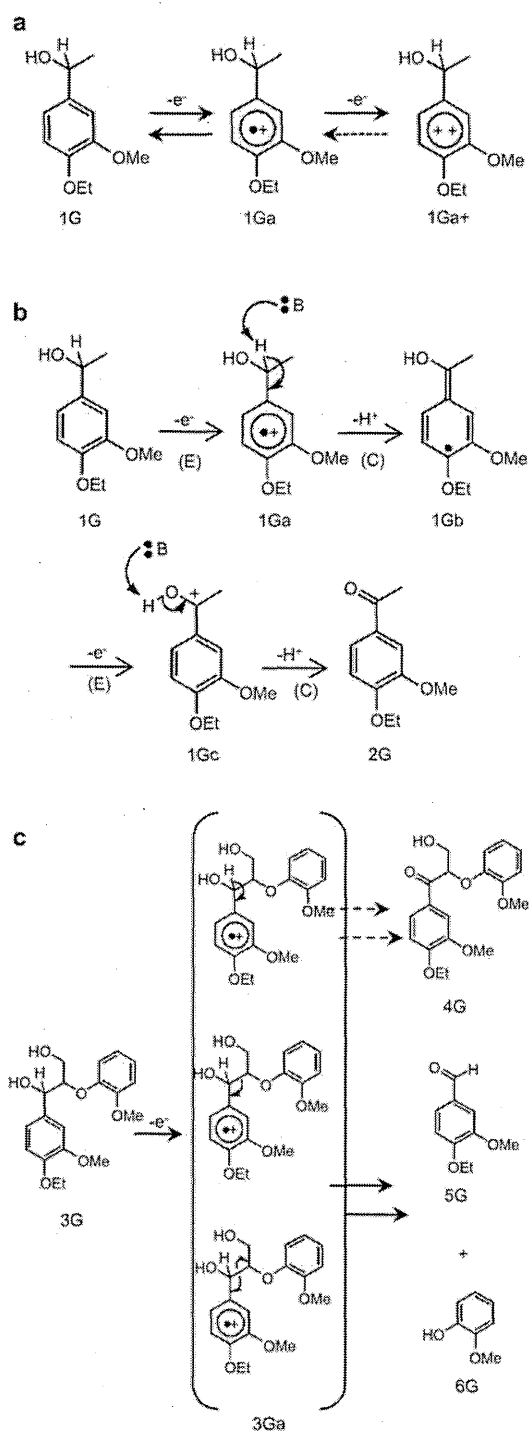
Figure 6 Proposed electron transfer and reaction mechanism for the compounds indicated (key in Figure 1). (a) Mechanism in the TFA system. (b) ECEC mechanism of compound 1G. (c) Reaction mechanism of compound 3G.

observations that radical cation 1Ga, which was formed by single-electron oxidation of compound 1G, was rapidly converted to an unknown intermediate, which is not 1Gb in the

ECEC mechanism described in Figure 6(b), and was rapidly oxidized further via single-electron oxidation at 1.1 V.

To obtain α-carbonyl compound 2G, the reaction should proceed via the ECEC mechanism presented in Figure 6(b), which consists of four steps: (E) first single-electron transfer step (first single-electron oxidation), (C) chemical step (deprotonation at Cα-H), (E) second single-electron transfer step (second single-electron oxidation), and (C) chemical step (deprotonation at Cα-OH). The deprotonation of radical cation 1Ga at Cα-H before the second single-electron oxidation seems to be important to form compound 2G via the ECEC mechanism. 2,6-Lutidine as a mild alkaline compound is known to be a catalyst in the electrooxidation of lignin model dimers (Pardini et al. 1991). This is the reason why 2,6-lutidine was added to the system to accelerate deprotonation. Figure 2 (C, D) shows CV of compounds 1G and 2G in 0.1 M LiClO₄/CH₃CN with 2,6-lutidine (5.0 eq of the substrate). In the CV of compound 1G, the oxidation peaks (e) at 1.1 V and (f) at 1.4 V are perceptible. The latter corresponds clearly to the peak (g) at 1.4 V in the CV of compound 2G, indicating that compound 2G is formed in the system with 2,6-lutidine. The current of the former was approximately same as that of peak (a) at 1.1 V in the system without a catalyst. The interpretation is that single-electron oxidation occurred twice at that potential. As expected, this result means that the conversion of radical cation 1Ga, which was formed by first single-electron oxidation, to 1Gb by deprotonation and the following second single-electron oxidation of 1Gb to 2G, proceeded rapidly in the presence of 2,6-lutidine.

Figure 4 (G, H) shows CV of compounds 1S and 1P in 0.1 M LiClO₄/CH₃CN without catalyst. The potentials of the oxidation peaks (h) and (i) of 1S and 1P were 1.1 V and 1.4 V, respectively (for comparison: 1.1 V for 1G). Thus, no significant difference was detected in oxidation potentials between non-phenolic guaiacyl and syringyl compounds. In contrast, in voltammetric studies of phenolic monoligols by Tobimatsu et al. (2008) and Bortolomeazzi et al. (2007) the potential of the first peak decreased with increasing numbers of methoxy groups, i.e., in the order P > G > S. The CV patterns of 1G, 1S, and 1P are different to some extent. The current of the low-voltage peak of 1S (h) is lower than that of 1G (a), while the current of 1P (i) is higher than that of 1G. These results indicate that different chemical reactions and a second oxidation occur after the first single-electron oxidation step in a system without a catalyst.

Figure 4 (I, J) shows the CVs of compounds 1S and 1P in 0.1 M LiClO₄/CH₃CN with 2,6-lutidine (5.0 eq of the substrate), respectively, in which the first (j, l) and second oxidation peaks (k, m) are visible. The latter peaks are in the range of the oxidation peaks of compounds 2S and 2P (data not shown). The current of the first oxidation peaks (j, l) is approximately the same as that of peak (e) in Figure 2 (C). The conclusion is that the reactions proceed via the ECEC mechanism, as expected.

Next, the bulk electrolyses of compounds 1G, 1S, and 1P were carried out in the system with 2,6-lutidine near the potential of the first oxidation peaks in their CVs, although

the potentials of 1G and 1S were slightly changed to prevent a further electrooxidation of the oxidation products 2G and 2S. The results are listed in Table 1.

The electrolysis of compound 1G in the presence of 2,6-lutidine (3.0 eq of the substrate) leads to 2G in 57.1% yield, while the yield increases with increasing amounts of 2,6-lutidine. The highest yield, 79.1%, was obtained with 2,6-lutidine (20.0 eq), but in the presence of 30.0 eq 2,6-lutidine no further yield increment was achieved. In any case, compound 1G was entirely consumed. In case of a bulk electrolysis of compound 1G without 2,6-lutidine as a control, the initial colorless anolyte turned to purple during electrolysis. Only a trace amount of compound 2G was detected in the anolyte after the electrolysis, although compound 1G was entirely consumed. The interpretation is that unknown side-reactions must have occurred preferentially, as expected based on the CV in Figure 2.

If the compounds 1S and 1P were oxidized in the presence of 2,6-lutidine, the yield of the resulting compounds 2S and 2P was elevated in the presence of 20.0 eq 2,6-lutidine to 61.7% and 75.3%, respectively. The yield of 2S is lower than those of compounds 1G and 1P. The reason might be that the reaction rate in deprotonation at C_α-H decreased in the ECEC mechanism by the electron-donating effect of the two methoxyl groups of the syringyl nucleus. Consequently, electrooxidation of compounds 1G, 1S, and 1P proceeds probably in the presence of 2,6-lutidine towards the corresponding α-carbonyl compounds 2G, 2S, and 2P in high yields.

The electrolysis of compound 1G was performed with bases, which have different pKa values to that of the corresponding conjugate acid. Pyridine (pKa: 12.3), 2,6-lutidine (pKa: 15.4) and 2,4,6-collidine (pKa: 16.8) were selected for this purpose. The yield of compound 2G increased with increasing pKa value, i.e., 2,4,6-collidine was found to be a better base than 2,6-lutidine. Also here, a rapid deprotonation at C_α-H in the ECEC mechanism was needed to obtain compound 2G.

Electrooxidation of the non-phenolic dimer 3G

The behavior of the non-phenolic β-O-4 dimer 4-ethoxy-3-methoxyphenylglycerol-β-guaiacyl ether (3G) was investigated. Two publications have dealt with the electrooxidation of a similar β-O-4 dimer (3,4-di-methoxyphenylglycerol-β-guaiacyl ether) without a catalyst. Pardini et al. (1992) reported that electrooxidation of the β-O-4 dimer at 50 mA in 0.1 M NaOMe/0.2 M $NaClO_4$/MeOH-CH_2Cl_2 (70/30=v/v) gives veratraldehyde in 35.0% yield. Obviously, C_α-$C_\beta$cleavage occurred. Rochefort et al. (2002) found that electrooxidation of the β-O-4 dimer at 0.9 V (vs. Ag/AgCl) in citrate buffer (pH 4.5) afforded C_α-carbonyl compound and veratraldehyde in 6.0% and 3.5% yields, respectively. Thus, C_α-$C_\beta$cleavage (aldehyde formation) and C_α-carbonylation must have proceeded simultaneously (Figure 6c). However, a direct comparison of the results in the quoted papers and those in the present study is difficult, as the electrooxidation conditions were critically different and the two reports did not present CVs.
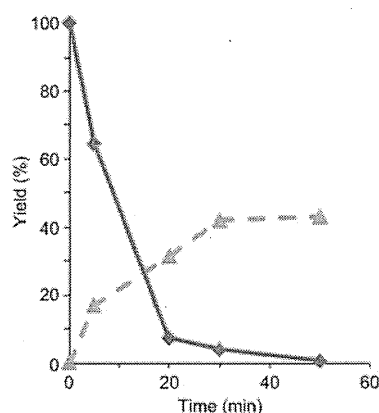
Figure 7   Reaction profile for electrolysis of compound 3G (electrolyte: 0.1 M $LiClO_4$/CH_3CN, electrolytic potential: 1.1 V vs. Ag/Ag^+). Dotted line: yield of the degradation product 5G (4-O-ethylvanillin).

Figure 5 (K) shows CV of compound 3G in 0.1 M $LiClO_4$/CH_3CN without a catalyst. In the CV, the first oxidation peak (n) at 1.1 V and second oxidation peak (o) at 1.5 V are present, whereas the oxidation peak at 1.3 V, which corresponds to the first oxidation peak (p) of compound 4G, is absent. Clearly, C_α-carbonylation did not occur, as was the case for the monomer 1G. A bulk electrolysis of compound 3G was also performed at 1.1 V (vs. Ag/Ag^+) during 60 min without catalyst. Compound 4G was not detected in the anolyte, but 4-O-ethylvanillin (5G) was found. The result is in agreement with that obtained under the conditions 0.1 M NaOMe/0.2 M $NaClO_4$/MeOH-CH_2Cl_2 (70/30=v/v) by Pardini et al. (1992). Figure 7 shows the reaction profile of 3G. The recovery yield decreases rapidly within 20 min and then slowly approaches 0%, whereas the yield of compound 5G (4-O-ethylvanillin) increases up to 30 min and levels off to 40%. An α-carbonyl compound 4G was not detected during the electrolysis. Accordingly, C_α-$C_\beta$cleavage of compound 3G preferentially occurs and yields 5G and an unknown reaction becomes prevalent.

Figure 5 (M) shows CV of compound 3G in 0.1 M $LiClO_4$/CH_3CN with 2,6-lutidine. The CV pattern is distorted and shoulders (q) and (r) at 1.1 V and 1.5 V, which apparently correspond to the oxidation peaks (s) and (t) of compound 4G, are not well pronounced. The oxidation peaks from the B-ring of compound 3G may be overlapped. The bulk electrolysis of compound 3G was carried out under similar conditions as described for compound 1G. Surprisingly, however, the current stopped within several seconds after starting. The anode was deactivated, but a film was not observed on the anode surface. The deactivated anode could be activated by washing with CH_2Cl_2. Any other compounds beyond the starting material 3G could not be detected by TLC analysis in the anolyte. The use of 2,4,6-collidine or pyridine instead of 2,6-lutidine gave the same results. The interpretation is that the electrode is passivated by an unknown rapid reaction in the vicinity of the anode. Electrode passivation by polymerization of phenolic compounds

is well established (Bruno et al. 1977; Parpot et al. 2000; Ezerskis and Jusys 2001). Thus, one explanation of these results may be that guaiacol (6G), which is a product of the C_α-C_β cleavage of compound 3G, was polymerized on the electrode surface. However, this hypothesis needs closer investigation.

Conclusions

It is understood that C_α-C_β cleavage (indicated by aldehyde formation) is a competitive reaction of C_α-carbonylation (C_α-deprotonation). In the electrooxidation of the monomeric model compounds 1G, 1S, and 1P at a constant potential in the system with 2,6-lutidine as alkaline catalyst, C_α-carbonylation preferentially proceeded and gave the corresponding C_α-carbonyl compounds 2G, 2S, and 2P, respectively. On the other hand, without a catalyst unknown reactions occurred. These results can be interpreted as acceleration of C_α-deprotonation of a radical cation intermediate by 2,6-lutidine in the ECEC mechanism (Figure 6b). However, in the electrooxidation of the dimeric compound 3G at a constant potential in presence of 2,6-lutidine, the reaction stopped unexpectedly after a short time, although in the reaction without a catalyst C_α-C_β cleavage took place to give 4-O-ethylvanillin (5G) in moderate yield. These results show the different electrochemical behavior of simple monomers and β-O-4 model dimers. It is concluded that direct electrooxidation is not suitable for the C_α-carbonylation of lignin. In the next paper, C_α-carbonylation of lignin model compounds by indirect electrooxidation with a mediator will be described.

Acknowledgements

References

Aoyagi, T., Hosoya, S., Nakano, J. (1980) Contribution of α-carbonyl groups to the degradation of lignin during oxygen-alkali cooking. Mokuzai Gakkaishi 26:27–30.

Baciocchi, E., Bietti, M., Lanzalunga, O. (2000) Mechanistic aspects of β-bond-cleavage reactions of aromatic radical cations. Acc. Chem. Res. 33:243–251.

Bortolomeazzi, R., Sebastianutto, N., Toniolo, R., Pizzariello, A. (2007) Comparative evaluation of the antioxidant capacity of smoke flavouring phenols by crocin bleaching inhibition, DPPH radical scavenging and oxidation potential. Food Chem. 100: 1481–1489.

Britton, W., Steelink, C. (1974) The electrochemical oxidation of lignin model compounds II. Oxidation of 3,5-dimethoxy-4-hydroxyacetophenone. Tetrahedron Lett. 33:2873–2876.

Bruno, F., Pham, M.C., Dubois, J.E. (1977) Polaromicrotribometric study of polyphenylene oxide film formation on metal electrodes by electrolysis of disubstituted phenols. Electrochim. Acta 22: 451–457.

Chabaud, B., Sundholm, F. (1978) Aniodic oxidation of some phenols related to lignin II. Oxidation of isoeugenol methylether and 4-propylveratrole in acetonitrile. Electrochim. Acta 23: 659–667.

Crestini, C., D'Auria, M. (1997) Singlet oxygen in the photodegradation of lignin models. Tetrahedron 53:7877–7888.

Ezerskis, Z., Jusys, Z. (2001) Electropolymerization of chlorinated phenols on a Pt electrode in alkaline solution Part I: A cyclic voltammetry study. J. Appl. Electrochem. 31:1117–1124.

Gierer, J., Ljunggren, S. (1979) The reactions of lignin during sulfate pulping Part 16. The kinetics of the cleavage of β-aryl ether linkages in structures containing carbonyl groups. Svensk Papperstidning 82:71–81.

Gierer, J., Norén, I. (1982) Oxidative pretreatment of pine wood to facilitate delignification during kraft pulping. Holzforschung 36:123–130.

Gierer, J., Ljunggren, S., Ljungquist, P., Norén, I. (1980) The reactions of lignin during sulfate pulping. Part 18. The significance of α-carbonyl groups for the cleavage of β-aryl ether structures. Svensk Papperstidning 83:363–369.

Hammerich, O., Parker, V.D. (1973) The reversible oxidation of aromatic cation radicals to dications. Solvents of low nucleophilicity. Electrochim. Acta 18:537–541.

Hosoya, S., Nakano, J. (1980) Reaction of α-carbonyl group in lignin during alkaline hydrogen peroxide bleaching. Mokuzai Gakkaishi 26:97–101.

Lalvani, S.B., Rajagopal, P. (1993) Hydrogen production from lignin-water solution by electrolysis. Holzforschung 47:283–286.

Limosin, D., Canquis, G.P. (1985) Étude électrochimique de quelques composes dimères modèles de la lignine. Holzforschung 39:91–98.

Limosin, D., Pierre, G., Cauquis, G. (1986) Oxidation electrochimique de quelques echantillons de lignine en solution aqueus basique. Holzforschung 40:31–36.

Ljunggren, S. (1980) The significance of aryl ether cleavage in kraft delignification of softwood. Svensk Papperstidning 83:363–369.

Ljunggren, S., Olsson, A. (1984) The specificity in oxidation of some lignin and carbohydrate models and pine wood shavings with permanganate and pyridinum dichromate before the kraft pulping process. Holzforschung 38:91–99.

Löbbecke, J.G., Lindner, A., Wegner, G., Wabner, G.W. (1990) Anodic modification of lignin during electrolysis in the organocell process. Holzforschung 44:401–406.

Nakatsubo, F., Sato, K., Higuchi, T. (1975) Synthesis of guaiacyl-glycerol-β-guaiacyl ether. Holzforschung 29:165–168.

Pardini, V.L., Smith, C.Z., Utley, J.H.P., Vargas, R.R., Viertler, H. (1991) Electroorganic reactions. 38. Mechanism of electrooxidative cleavage of lignin model dimmers. J. Org. Chem. 56: 7305–7313.

Pardini, V.L., Vargas, R.R., Viertler, H., Utley, J.H.P. (1992) Anodic cleavage of lignin model dimers in methanol. Tetrahedron 48: 7221–7228.

Parpot, P., Bettencourt, A.P., Carvalho, A.M., Belgsier, E.M. (2000) Biomass conversion; attempted electrooxidation of lignin for vanillin production. J. Appl. Electrochem. 30:727–731.

Rochefort, D., Bourbonnais, R., Leech, D., Paice, M.G. (2002) Oxidation of lignin model compounds by organic and transition metal-based electron transfer mediators. Chem. Comm. 11: 1182–1183.

Sawyer, D.T., Sobkowiak, A., Roberts, J.L. (1995) Electrochemistry for Chemists, 2nd Edn. Wiley, New York.

Sjöblom, K. (1996) Extended delignification in kraft cooking through improved selectivity. Nord. Pulp Pap. Res. J. 11:177–185.

Smith, C., Utley, J., Petrescu, M., Viertler, H. (1989) Biomass elec-
trochemistry: anodic oxidation of an organo-solv lignin in the
presence of nitroaromatics. J. Appl. Electrochem. 19:535–539.

Steelink, C., Britton, W. (1974) The electrochemical oxidation of
lignin model compounds I. Oxidation of 3,5-dimethoxy-4-
hydroxy-α-methylbenzyl alcohol. Tetrahedron Lett. 33:2869–
2872.

Sundholm, F. (1982) Anodic oxidation as a tool for mechanistics
studies, guaiacol and 4-propyl-guaiacol in aprotic media. Holz-
forschung 36:7–74.

Tobimatsu, Y., Takano, T., Kamitakahara, H., Nakatsubo, F. (2008)
Studies on the dehydrogenative polymerizations of monolignol
β-glycosides. Part3: Horseradish peroxidase-catalysed polymer-
izations of triandrin and isosyringin. J. Wood Chem. Technol.
28:69–83.